Electrical Engineering
https://doi.org/10.1007/s00202-022-01592-7

ORIGINAL PAPER

Common and differential mode of dc-bias in three-phase power transformers

Wei Wang[1] · **Arne Nysveen**[1] · **Niklas Magnusson**[2]

Received: 17 February 2021 / Accepted: 9 June 2022

Abstract
Dc magnetization due to the geomagnetically induced currents (GICs) and HVDC (High Voltage Direct Current) systems may cause core saturation and result in serious destruction in the transformer performance as well as the power system stability. Based on susceptibility, transformers are classified into different groups. For instance, a three-phase, three-limb transformer is considered less vulnerable to effects of GIC compared to a single-phase or a three-phase, five-limb transformer. However, our study shows that such classifications do not apply to the dc magnetization caused by converter modulation. In this article, we introduce the concept of common mode and differential mode to distinguish dc-bias caused by different mechanisms. Main focus is given on differential mode dc current since it has rarely been reported in any literature. The differential mode dc current was demonstrated by system simulations of classic three-level voltage source converters as well as modular multilevel converter. Detailed experimental investigations were made on a three-phase, three-limb transformer, where the loss impact as well as reactive power consumption were studied. The test shows a significant difference in stray loss between the two modes in three-phase power transformers. Finally, we discuss the effect of delta winding on dc-bias of different modes.

Keywords AC-DC power converters · Dc magnetization · Geomagnetically induced current · HVDC transmission · Transformers · Saturation magnetization

1 Introduction

Geomagnetically induced currents (GICs) [1–4] and HVDC system operation [5–9] are two main causes of dc magnetization in power transformers. It is well known that dc magnetization can lead to half-cycle saturation of the transformer core, and adversely affect the performance of the power transformer as well as the power system [4]. The excessive magnetization current can create hot spots in windings and structural parts [10], increases reactive power absorption and cause voltage instability [11]. In the worst scenario, the destruction of grid transformers [12] and system blackouts [13] may occur due to dc magnetization. To eliminate dc currents, mitigation measures often involve substantial investments such as in dc blocking devices [14] for GIC or fundamental frequency blocking filters [15] for the converter related dc currents.

GIC is associated with the phenomenon of geomagnetic disturbance (GMD). The coronal mass ejections (CME) originated from the sun interacts with the magnetosphere of the earth and induce a longitudinal quasi-dc potential on the transmission lines, which drives the flow of GICs [4]. The quasi-dc current flow in the ground via the star windings of the grid transformer at the grounded neutral points. Since the directions of the currents in the three phases are identical, those currents are often referred as zero sequence.

HVDC systems can introduce dc currents into power transformers in two ways. The stray dc current due to HVDC electrode operations (monopolar or bipolar operation) can flow into solidly earthed transformers between two substations. This dc current can have two major consequences: saturation of the grounded transformers and corrosion of the ground grid of the station nearest the cathode [8]. Mitigation schemes are extensively discussed in [16].

Another major cause of dc magnetization by HVDC systems is the modulation effect of power converters. A rapid increase in the number of HVDC transmission lines creates

✉ Wei Wang
weiwan@ntnu.no

[1] Norwegian University of Science and Technology, NO-7491 Trondheim, Norway

[2] SINTEF Energy Research, NO-7465 Trondheim, Norway

Published online: 11 July 2022

a situation where ac and dc lines may share the same corridor or even share the same towers [6, 7]. A neighboring ac line can induce a substantial fundamental current onto the dc line. The induced fundamental voltage and current on the dc side of the converter will then transfer to the ac side and appears as a dc-bias [5]. Parameter sensitivity study on the coupling effect has been reported in [7, 17], where the parallel length, separation distance between ac/dc lines, line transposition and ground resistivity are discussed. Literature [17] focuses on VSC-HVDC transmission system, where a frequency domain model is derived for parameter sensitivity study. With the equivalent impedance representation of the network, the factors such as dc capacitors and modulation index are studied analytically.

Since 1989, when the blackout due to GIC occurred in Canada [13], the phenomenon has been drawn significant attention. The guideline [4] has classified power transformers into four groups based on their susceptibility to effects of GIC and has been widely used for selecting or validating power transformers subjected to dc current. However, as comparison, we will demonstrate that the feature of the dc current generated by converter modulation is significantly different from GICs and the stray current introduced by HVDC electrode operations. First, GICs are characterized by a large number of narrow consecutive pulses over a period of hours separated by a few high peak pulses of less than a few minutes duration [4]. In contrast, the dc currents generated by HVDC systems (either by converter modulation or by electrode operation) are mostly constant. Another important difference, which has not been addressed in any literature, is the directions of the dc currents in three phase windings. GICs and the stray dc current introduced by HVDC systems are well known to be of zero sequence, whereas, this is not the case for the dc current generated by converter modulation.

In this article, we investigate the performance of a three phase, three-limb transformer, subjected to different types of dc currents. Main focus will be given on the modulation related dc currents due to the lack of research and understanding of this phenomenon. First, we analyze the modulation effect in voltage source converters (VSCs) and demonstrate the dc current distribution in the three phases. Then, we introduce the concept of common mode and differential mode to distinguish dc-bias of different directions. By experiment, we compare the loss impact as well as reactive power variation in three-phase power transformers of the two modes. Last, we discuss the effect of delta winding on dc-bias of different modes.

2 Modes of dc-bias in power transformers

To distinguish dc currents generated by different mechanisms, we introduce *common mode* (CM) for GICs and stray currents, and *differential mode* (DM) for converter modulation related dc current, based on their current directions. System-oriented models are developed to demonstrate dc current introduced by the modulation effect.

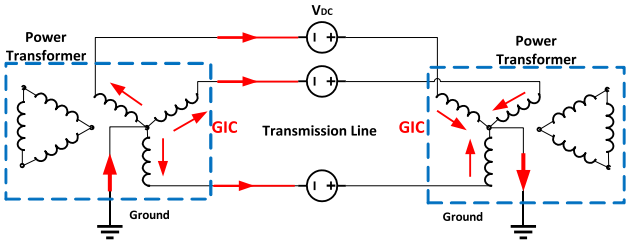

Fig. 1 Geomagnetically induced current distribution in three-phase power system and power transformers

2.1 Common mode

The scenario of GIC generation in the network is depicted in Fig. 1. GIC is a quasi-dc current (low frequency, typically 0.01 Hz to 0.5 Hz) that flows in the power system, closing its path through transmission lines, windings and neutral points of grid transformers and ground. Factors that influence the level of GIC include geomagnetic latitude, ground resistivity, network topology and the design of the power transformer. In spite of its destructive impact, high level GICs can hardly sustain over a long period. Often, the peak pulses have time constant less than a few minutes, which is smaller than the thermal time constant of the magnetic core (typically in a range of half hour), but larger than the thermal time constant of the structural steels. Therefore, the thermal issue caused by GIC is mostly related to the hot spots caused by stray flux, not the overall power loss.

Different from GICs, the stray currents are driven by the potential difference between substations due to HVDC electrode operation. That is, the current emanating from the anode partly enters the earth of one substation and flows into the grounded neutrals of the transformer towards the other substation (and the cathode) [8]. Apart from the difference in origination, the stray currents feature a stationary dc current. Therefore, a peak pulse specification is not as crucial as GICs.

Regardless of the differences between the two mechanism, stray dc currents due to HVDC electrode operation are similar to GICs: the dc currents are in the same direction in all three phases. At very low frequencies, the high-voltage network is essentially resistive. Considering the symmetric resistance in three phases, the magnitudes of dc currents in three phases are practically equal. Based on these factors, the GICs and the stray currents are classified as CM.

Several factors determine the susceptibility of the power transformer to CM dc current, such as core topology, winding configuration, and the design of structural parts. Among

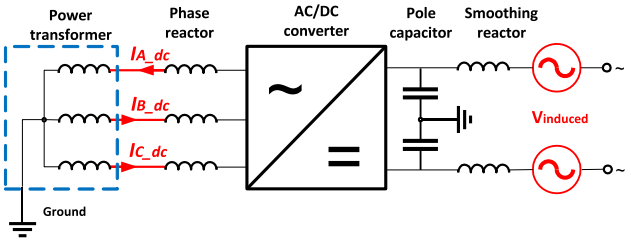

Fig. 2 Fundamental frequency voltage and current on the dc side of the VSC-HVDC converter transfer to the ac side and appear as dc current circulating in the windings of the power transformer

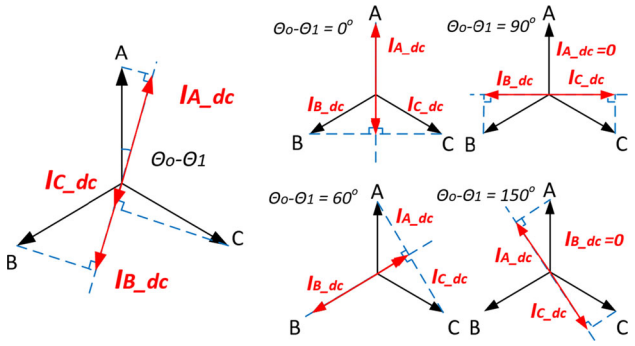

Fig. 3 Phasor representation of the dc component in each phase of the transformer winding due to the modulation effect. $\theta_0 - \theta_1$ determines the magnitudes of dc current in each phase. The scenarios 0°, 60°, 90° and 150° will be investigated in detail

them, the core topology has a major impact on the classification. Single-phase and five-leg core transformers providing low reluctance path for the dc flux, are susceptible to saturation. The three-phase, three-limb transformer, on the other hand, is less susceptible to core saturation due to the high reluctance path for dc flux. In a three-phase, three-limb transformer, the CM flux must pass through the path from the top yoke to the tank top, through the tank walls, and return to the bottom yoke from the tank bottom.

2.2 Differential mode

A dc line in parallel with an ac line is exposed to an inductive coupling. A longitudinal voltage potential of fundamental frequency is induced along the dc line. As depicted in Fig. 2, the induced fundamental frequency voltage and current on the dc side of the converter transfer to the ac side and appear as a dc current (and second-order harmonic) circulating in the windings of the power transformer.

The inductive coupling part is represented as two longitudinal voltage sources in this model. The difference between two voltage sources and the impedance seen from dc side determines the dc current level on the ac bus. Different from CM, the sum of the dc currents appearing on the ac bus is zero. Thus, it is referred as differential mode (DM). As the dc currents are not identical in the three phases, the magnetization of the transformer core becomes non-symmetric. Likewise, the saturation caused by DM dc current can result in excessive heating and an increased noise level in the transformer.

The distribution of the dc currents among the three phases depends on the phase difference between the induced voltage sources and the switching operation. However, this information is not controllable since the two systems do not have to be synchronized. For simplicity, we assume that two fundamental frequency voltage sources u_p and u_n have the same magnitude V_m but are out of phase:

$$\begin{cases} u_P = V_m \cos(\omega_0 t + \theta_0) \\ u_n = -V_m \cos(\omega_0 t + \theta_0) \end{cases} \tag{1}$$

where ω_0 is the fundamental frequency and θ_0 is the phase of the induced voltage source.

The voltage on the ac bus of the converter can be expressed in terms of switching functions [5]:

$$u_{ac} = S_p \times u_p + S_n \times u_n \tag{2}$$

where the switching functions S_p and S_n of the converter are defined as:

$$\begin{aligned} S_p &= \frac{1}{2}\begin{bmatrix} 1 + m\cos(\omega_0 t + \theta_1) \\ 1 + m\cos(\omega_0 t + \theta_1 - \frac{2}{3}\pi) \\ 1 + m\cos(\omega_0 t + \theta_1 + \frac{2}{3}\pi) \end{bmatrix} \\ S_n &= \frac{1}{2}\begin{bmatrix} 1 - m\cos(\omega_0 t + \theta_1) \\ 1 - m\cos(\omega_0 t + \theta_1 - \frac{2}{3}\pi) \\ 1 - m\cos(\omega_0 t + \theta_1 + \frac{2}{3}\pi) \end{bmatrix} \end{aligned} \tag{3}$$

where m is the modulation index and θ_1 is the phase of the switching function.

By inserting (1) and (3) into (2), taking only the dc component of (2) u_{dc} and by simplifying, we obtain:

$$u_{\mathrm{dc}} = \frac{m V_m}{2}\begin{bmatrix} \cos(\theta_1 - \theta_0) \\ \cos(\theta_1 - \theta_0 - \frac{2}{3}\pi) \\ \cos(\theta_1 - \theta_0 + \frac{2}{3}\pi) \end{bmatrix} \tag{4}$$

Equation (4) indicates that the relative phase difference between the induced voltage and the switching function of the converter $\theta_0 - \theta_1$ determines the magnitudes in each phase. A phasor interpretation of (4) is described in Fig. 3.

Since the relationship between the phase of induced voltage θ_I and the phase of the switching function θ_0 is unknown, the magnitudes among three phases varies. To identify the worst case in terms of power losses, we define four scenarios where the phase difference varies from 0 to 150° as illustrated in Fig. 3. Note that the dc current magnitudes of 0° and 90°

Table 1 Dc current defined in each phase of the transformer

$\theta_0 - \theta_1$		Dc current ratio in phase A, B and C				Ref. range [A]
		I_{A_dc}	I_{B_dc}	I_{C_dc}	I_0	
DM	0°	1	− 0.5	− 0.5	0	0.4–1.6
	60°	0.5	− 1	0.5		
	90°	0	$-\sqrt{3}/2$	$\sqrt{3}/2$		
	150°	$-\sqrt{3}/2$	0	$\sqrt{3}/2$		
CM	/	1	1	1	3	0.4–4.0

The applied current in each phase is the multiplication of the current ratio and Ref. range

are the same as 60° and 150°, but distribute in different limbs (the flux path of the middle limb and the side limb are different in a three-phase transformer). To compare the difference between DM and CM, we also define test cases of CM where the dc currents in the three phases are in the same direction. The tests are conducted for a three-phase, three-limb transformer. The ratio and the range of the current applied are listed in Table 1.

In the system study, we made simulations with the setup described in Fig. 2, a classic three-level voltage source converter model and a modular multilevel converter (MMC) [18] model with full control function implemented. The models were built in MATLAB®/Simulink® [19]. The 200 MVA three-level VSC uses Neutral Point Clamped (NPC) topology and Sinusoidal Pulse Width Modulation (SPWM) scheme. On the ac side, the station includes a 230 kV step-down Yg-D transformer and filters. The 150 MVA 12-level MMC levels uses cascaded two-level topology and nearest level control [18]. No filter or smoothing reactor is included in MMC as the harmonic level has been well managed. In both models, the transformers were modeled in a simply way, i.e., tap changers and saturation characteristics were not simulated since the purpose for the simulation was to demonstrate the modulation effect of the power converters. The main circuit parameters for the two converters are summarized in Table 2.

The phase currents on the ac of the converter bus as well as their dc components obtained from the simulations are demonstrated in Fig. 4.

The induced longitudinal fundamental frequency voltage on the dc side causes the unbalanced phase currents on the converter ac buses, as they contain dc component of different levels and directions in each phase. The dc (component) current circulates within three phases and the sum of them must be zero. This modulation effect occurs in both three-level VSC and MMCs, where the dc currents generated in MMCs has less ripple than in three-level VSCs.

Compared to the pulsating nature of GIC, the induced dc current is considered to be more constant (in both direction

Table 2 Main circuit parameters of the converters

Main circuit parameters	Unit	Three-level VSC	MMC
Converter rating	MVA	200	150
System frequency	Hz	50	50
DC voltage	kV	+ /_ 100	+ /_ 200
AC voltage	kV	230	123
AC filter size	MVar	40	/
Reactance of phase reactor	mH	23.9	50.9
Converter bus voltage	kV	100	123
Transformer rating	MVA	200	150
Transformer leakage reactance	mH	23.9	25.5
Reactance of smoothing reactor	mH	8	/

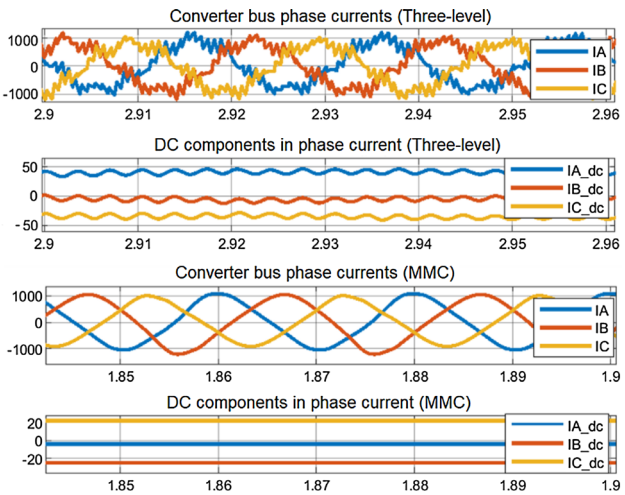

Fig. 4 Phase currents (IA, IB and IC) and their dc components (IA_dc, IB_dc and IC_dc) on the converter ac bus due to harmonic transfer from the dc side. The upper two figures are the result of the three-level VSC and the lower two figures are the result of MMC

and magnitude) as the (phase) regulation of the converter control does not change very often. As a result, a temperature rise can build up in the transformer. Therefore, both the overall power loss (in the core, windings and structural parts) and the located stray loss shall be evaluated for converter modulation related DC magnetization.

Although the mechanism of harmonic transfer is not the scope of this study, we must emphasize the importance of control implementation in the resultant dc current, as it has not been addressed in any literature. Converter internal impedance seen from the dc side is strongly affected by the converter controls and associated bandwidths, particularly in voltage-source converters. For example, the circulating current control (and/or any low-pass active filtering) used in MMCs behaves like a resistor seen from the induced voltage source. Therefore, the dc current derived by the analytical approach [17] without considering control effects may not be valid in practice. Nevertheless, in the following investigation, the dc current level on the ac converter bus is pre-defined and we study the influence of different modes on the power transformer.

Fig. 5 Test setup. 2.5 kVA three-phase, three-limb transformer for dc-bias test with (upper right) and without (upper left) iron tank. The EGSTON grid emulator (in National Smart Grid Laboratory operated by Norwegian University of Science and Technology and SINTEF Energy) provides controllable voltage source (lower)

3 Test

3.1 Test setup

A 2.5 kVA three-phase, three-limb transformer was used as the test object (Fig. 5), which is connected to the FPGA-based grid emulator (EGSTON®). The EGSTON grid emulator is a 200 kW switching voltage source converter with high bandwidth able to emulate a power system as ac/dc sources. In this test, it is important to program a symmetric ac source with independent, controllable dc components, such that the dc currents are tuned precisely to the predefined values, while the ac voltage is maintained to the nominal values.

Although the phenomenon under investigation is mainly related to grid and distribution transformers, the laboratory transformer is still adopted in our test because:

- The test can be destructive due to extreme saturation condition and excessive losses.
- It is easier to manufacture, modify and assembly iron tank to investigate stray losses.
- The conclusion drawn from a scale-down lab transformer is valid for a lager transformer since the saturation phenomenon is sensitive to materials and dimension ratio, rather than absolute dimensions.

The tank and the clamping plates are made of ordinary carbon steel. The electrical connections are well maintained (no air gap) when connecting the iron plates. The iron tank and the clamping plates can be disassembled such that the core and the stray (in the tank and the clamping steels) losses could be separated. Moreover, the height of the tank (i.e., the distance between the magnetic core and the cover/bottom) was adjustable such that the influence of geometry on stray loss in the tank could be further evaluated.

The number of turns was 280 for both the primary and the secondary windings of the transformer. The primary windings were connected (in star) to a three-phase power converter (three-phase power source, Fig. 6), which provided independent voltage sources for the three phases. The dc voltage bias of each phase was adjusted individually to make the currents reach the predefined values in Table 1. The secondary windings were connected in delta. A switch was used (Fig. 6) such that the impact of open circuit and delta connection could be investigated. No load is connected on the secondary side in the tests (Sect. 3.2, 3.3, 3.4). The current and the voltage in each phase were measured and incorporated into a high precision power analyzer to obtain the power losses and the reactive powers.

3.2 Common mode test

The dc voltage offsets in all three phases were tuned to the same magnitude and direction, where dc currents are CM. The ac nominal voltage (230 V_{rms}) was applied on the primary winding, and the dc voltage offsets were adjusted until

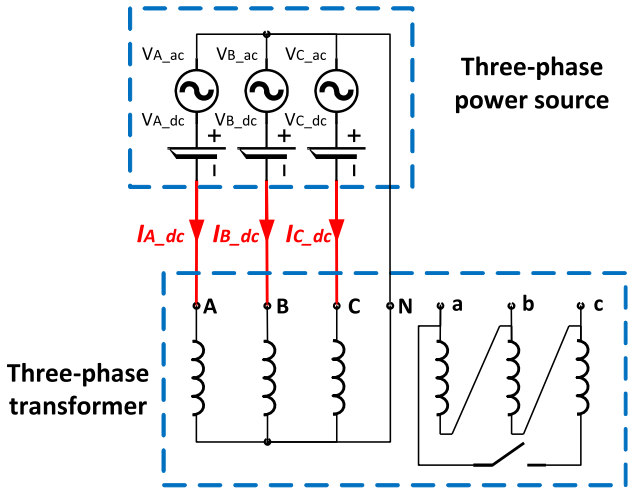

Fig. 6 Transformer winding connection and dc-bias implementation. The primary windings of the transformer were connected to a three-phase power source, where the dc voltage bias of each phase can be tuned. The switch was used to open the secondary delta winding

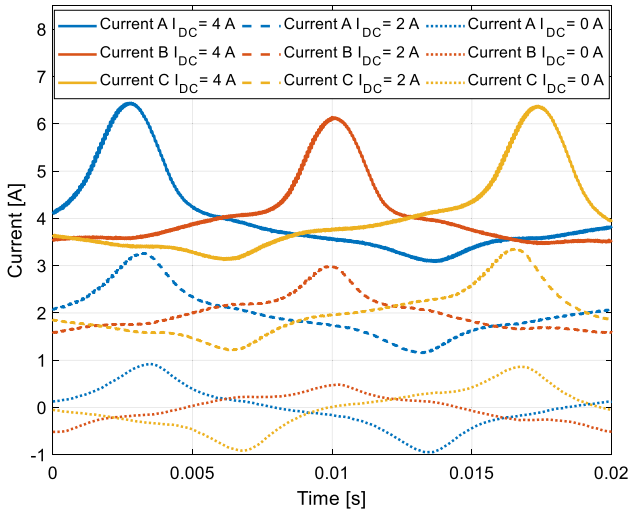

Fig. 7 The measured primary side (magnetizing) currents with different levels of CM dc component

the dc currents reached the preset values in Table 1 (from 0.4 to 4 A).

The measured total power losses consist of core loss, winding loss and stray loss. The winding loss was derived from the obtained current measurement and winding resistance. The core loss was obtained by withdrawing the winding loss from the total loss measured without the tank and the clamping structure. The stray loss was then derived by withdrawing the winding loss and the core loss from the measured total loss. The measurement results are given in Table 3.

The total power loss and the reactive power consumption increase significantly as the dc current increases. Although the core loss constitutes most in the power losses, the majority of the loss increase is from the winding loss, whereas the stray loss increases slightly and the core loss remains almost constant (the variation < 2%). This confirms the theoretical analysis in Sect. 2.1, namely the three-phase, three-limb transformer has a high reluctance path for the dc flux in CM and it is invulnerable to CM dc current.

Figure 7 shows the measured primary currents over one period at three different levels of dc-bias, i.e., 0 A, 2 A and 4 A. The average current in each phase is equal to the pre-defined dc currents. Without dc-bias (0 A), the average current is zero over a cycle. With dc current, there is a half-cycle asymmetry in the current waveform, which is more notable at 4 A than at 2 A. Moreover, there is an asymmetry in the three phases regardless of the dc current level. This is due to the difference in the reluctance between flux path in phase B (middle) and phase A and C (sides). Nevertheless,

Table 3 Power Losses and Reactive Power due to Dc-bias of CM

DC current [A]	Total losses P_t [W]	Winding loss P_w [W]	Core loss P_C [W]	Stray loss P_s [W]	Reactive power Q [Var]
0	51.02	0.20	50.06	0.76	260
0.4	51.32	0.51	50.05	0.77	386
0.8	52.15	1.31	50.05	0.79	615
1.2	53.33	2.52	50.02	0.81	876.8
1.6	55.04	4.26	49.95	0.84	1140.2
2.0	57.38	6.58	49.93	0.87	1417.7
2.4	60.20	9.36	49.92	0.92	1691.6
2.8	63.57	12.67	49.85	1.06	1971.1
3.2	67.62	16.48	49.81	1.31	2245.4
3.6	72.30	20.93	49.78	1.60	2530.9
4.0	77.54	25.86	49.74	1.95	2813.4

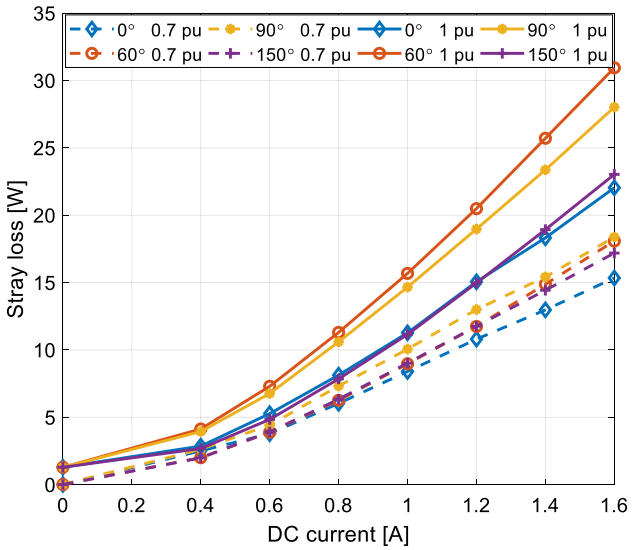

Fig. 8 Stray loss versus dc-bias level under 0.7 p.u. and 1 p.u. ac nominal voltages for four DM configurations

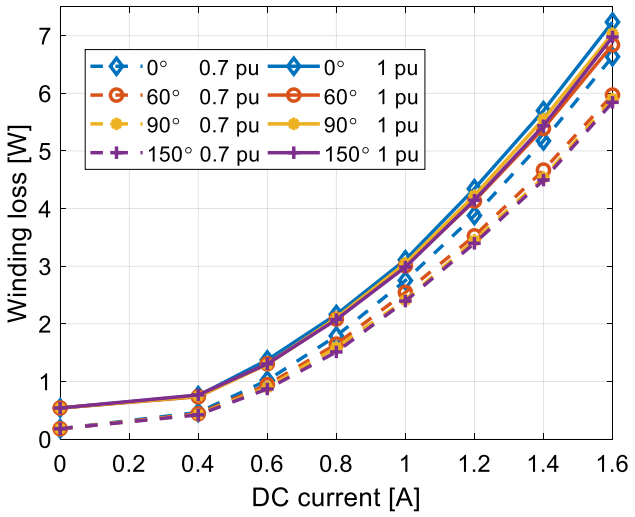

Fig. 9 Winding loss versus dc-bias level under 0.7 p.u. and 1 p.u. ac nominal voltages for four DM configurations

the half-cycle asymmetry in the waveforms of the magnetizing current is rather moderate under the applied CM dc current and transformer core does not reach saturation.

3.3 Differential mode test

The DM dc-bias in the three phases was implemented according to the definition in Table 1. The nominal ac voltage 230 V_{rms} (1 pu, corresponding to 1.48 T core flux density) and a lower voltage 161 V_{rms} (0.7 pu, corresponding to 1 T core flux density) were applied on the primary winding. The dc voltage offsets were adjusted until the dc currents reached the preset values in Table 1 (from 0.4 to 1.6 A). The power losses and the reactive power assumptions of four configurations were measured. The stray losses and the winding losses are shown in Figs. 8 and 9 respectively. Note that, for all the test cases, the measured core losses remain almost constant (< 2.5%); therefore, they are not demonstrated in detail in the following sections.

Unlike the CM dc current, the stray loss becomes very sensitive to the DM dc current due to the low reluctance path of the dc flux. As seen from Fig. 8, a dramatic loss increase can be observed as the dc-bias increases. In contrast, the power loss under CM dc current of the same levels are order-of-magnitude lower than that of DM.

Furthermore, there is a significant difference in the stray loss among the four configurations. This difference is smaller at lower ac voltage or lower dc current. And, the difference expands as the dc current increases. At the highest dc-bias level (1.6 A), the difference approaches 41% at the nominal ac voltage and 20% at 0.7 pu of nominal ac voltage. The highest stray loss (31 W) occurs when the largest dc current

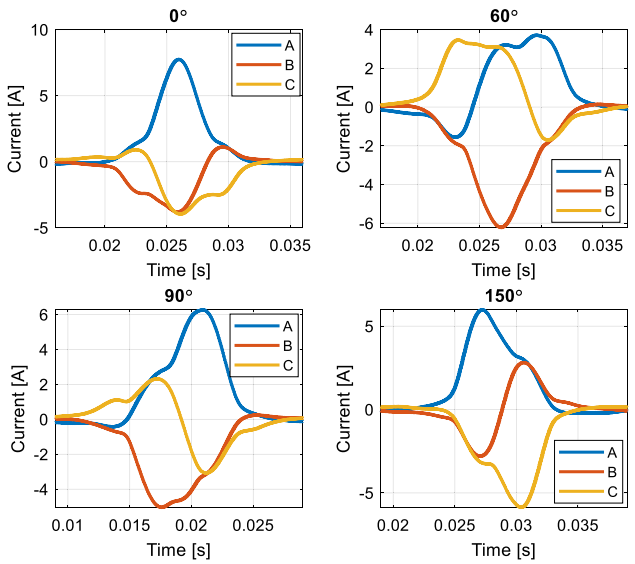

Fig. 10 The measured primary phase currents at different configurations of DM dc currents

is in the middle limb (i.e., 60°) and the lowest loss (22 W) occurs when the largest dc current is in the side limbs (i.e., 0°). The winding loss (Fig. 9) is highest for the 0° case, although the difference is not as notable as the stray losses.

Figure 10 shows the measured primary (magnetizing) currents over one period for the four configurations when the dc current is 1.6 A. Since no current flows in the neutral, the sum of the three-phase currents is zero. The peak values of the currents in DM are significantly larger than that of CM. Among four configurations, the 0° case gives the highest peak current (as well as the highest RMS current) at phase A, resulting in the highest winding loss (Fig. 9).

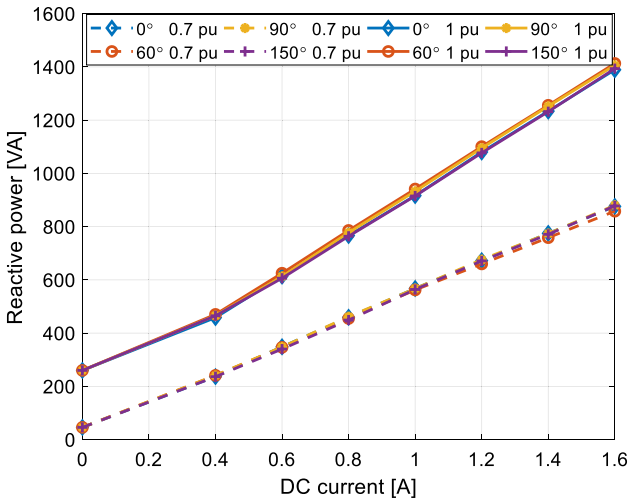

Fig. 11 Total reactive power consumption due to different levels of DM dc currents

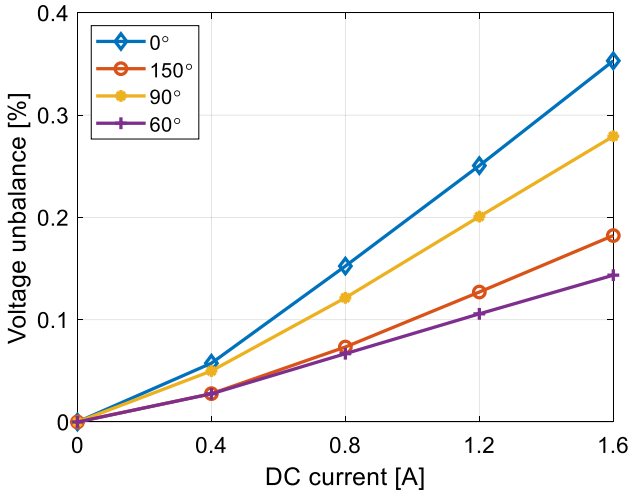

Fig. 12 Voltage imbalance due to different levels of DM dc currents

Table 4 Reactive Power due to a 1.6 A Dc-bias in DM

Configuration	Reactive power consumption [Var]			
	Phase A	Phase B	Phase C	Total
AC	133.7	83.5	109.1	326.3
0°	658.8	367.7	362.7	1389.2
60°	415.9	588.5	408.7	1413.1
90°	579.0	518.4	308.9	1406.3
150°	547.3	304.4	541.9	1393.6

Compared to the CM dc current, the magnetizing currents of DM have higher amplitudes and shaper spikes (i.e., higher-order harmonic content). Hence, it leads to the higher winding losses.

Different from the rapid increase in power losses (Figs. 8 and 9), the reactive power is practically linear with the dc current (Fig. 11), with little difference between the four configurations.

Although the total reactive power consumption is similar for the four configurations, the reactive power distributions in the three phases are significantly different for each configuration. An example of the reactive power distribution is given in Table 4, for a dc current of 1.6 A. Among the four configurations, the 0° case gives the largest difference between the three phases, which implies the largest voltage imbalance occurring in this scenario. The voltage imbalance (defined as ratio of the negative sequence fundamental voltage and the positive sequence fundamental voltage) of the four DM configurations with respect to different dc current level is shown in Fig. 12. A linear dependence on dc current can be observed and the case 0° gives the largest voltage imbalance.

3.4 Influence of tank and clamping steels

The measurement cases in Section IIIC were repeated after adjustment of the tank and the clamping structure, where the tank height (determined by the distance between the upper yoke and the tank cover and between the lower yoke and the tank bottom, d) was adjusted. Four cases were defined:

- Case 1:$d = 5$ mm.
- Case 2: $d = 20$ mm.
- Case 3: Without tank.
- Case 4: Without tank and clamping plate.

The loss measured in Case 4 equals the core loss (plus winding losses) since no tank and clamping structure were involved. The difference between Case 3 and Case 4 is due to the stray loss from the clamping plates. The difference between Case 1 (or 2) and Case 3 is the stray loss from the tank [20]. The results at a dc current of 1.6 A are given in Table 5.

As expected, both the tank and the clamping structure have a great impact on the stray loss. The loss in those structural parts largely attributes to eddy currents generated in proximity of the magnetic core. Several conclusions can be drawn from Table 5.

- The stray loss in the tank and the clamping plates increases dramatically due to dc-bias. In case 2, for instance, it increases from 1.3 (under pure ac excitation) to 31.3 W (1.6 A dc-bias at 60°).
- Among the four configurations, the stray loss varies considerably. The variations in Case 1 (33%) and Case 2 (37%) are greater than in Case 3 (26%), largely due to the stray loss redistribution in the iron tank.

Table 5 Power Losses due to Dc-bias of DM

Loss type	Configuration	Case number			
		1	2	3	4
Stray loss [W]	AC	1.9	1.3	1.2	0
	0°	32.5	22.8	7.7	0
	60°	43.3	31.3	9.7	0
	90°	40.4	28.7	8.4	0
	150°	34.5	24.3	8.4	0
Winding loss [W]	AC	0.4	0.4	0.4	0.4
	0°	7.2	7.2	7.4	7.7
	60°	6.9	6.8	6.9	7.1
	90°	7.0	7.0	7.0	7.4
	150°	6.9	7.0	7.0	7.3

- The stray loss in the tank is sensitive to the tank height (air gap). The loss increases with more than 10 W (> 40%) when the gap distance reduces from 20 to 5 mm.
- The winding loss increases with dc-bias level. The tank and clamping structures have little impact on winding loss.

In all measurement cases, the tank and the clamping structure have a minor influence (< 5%) on the reactive power.

3.5 Influence of delta winding

Delta connection is widely used in many types of three-phase transformers. Except for being used as a secondary winding, in high rating transformers, a delta connected tertiary winding can be used to reduce the unbalancing currents or to supply an auxiliary load at different voltage levels. The measurement Cases 1, 3 and 4 in Sect. 3.4 were repeated with the secondary winding connected in delta. The results at a dc current of 1.6 A are given in Table 6.

The delta winding significantly reduces the power loss caused by the dc-bias. The majority of the decreased loss is from the stray loss in the tank (> 25 W). Additionally, there is a reduction in the stray loss in the clamping structure (< 4 W), whereas the core loss is practically unchanged. Moreover, with delta winding, the loss difference between the four configurations becomes smaller. The winding loss in the primary side increases slightly with connecting the delta winding, due to the small increased magnetizing current. Last but not the least, in our test, the loss in the delta winding is moderate. However, in practice, attention should be paid to the rating of the delta winding as the induced current might exceed the design value. For instance, a delta winding used as tertiary winding supplying an auxiliary load might not be rated high enough to withstand the induced current caused by high dc bias.

Table 6 Power Losses due to Dc-bias of DM with Delta Winding

Loss type	Configuration	Case number		
		1	3	4
Stray loss [W]	0°	6.3	5.6	0
	60°	5.9	6.3	0
	90°	5.6	5.5	0
	150°	6.1	5.8	0
Winding loss primary side [W]	0°	7.7	7.8	7.9
	60°	7.3	7.3	7.4
	90°	7.4	7.4	7.6
	150°	7.3	7.3	7.4
Winding loss delta [W]	0°	1.7	1.7	0.9
	60°	2.2	2.3	2.0
	90°	2.0	2.0	1.5
	150°	1.6	1.5	0.7

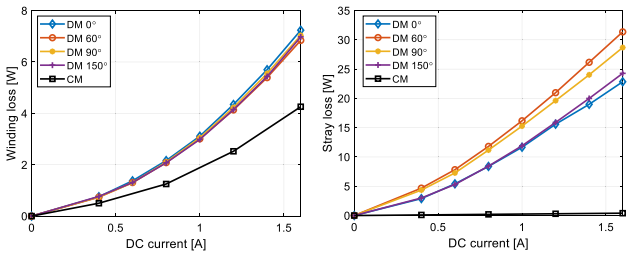

Fig. 13 Winding losses and stray losses due to different levels of DM and CM dc currents. Left: winding losses; Right: stray losses

The measurement were also repeated for CM dc currents. Since the core was not saturated under the applied CM dc current, no significant difference in the losses (core loss, winding loss and stray loss) was observed by adding a delta winding.

4 Discussion

4.1 Comparisons between DM and CM dc current

Comparisons of the power losses for DM and CM dc current are summarized in Fig. 13. Both the winding losses and stray losses of DM are significantly larger than those of CM.

The difference in winding losses can be explained by current total harmonic distortion (THD) of two modes. As an example, in Fig. 14 (DM case 0°), the THD of DM is significantly larger than CM. The harmonic currents account for considerable portion of the winding loss for DM. In contrast, the THD is small and increases very slightly for CM dc current, in which the winding losses is dominated by dc ohm loss. It is also worth noting that the winding losses distribution among three phases can be unbalanced due to asymmetric DM dc current distribution.

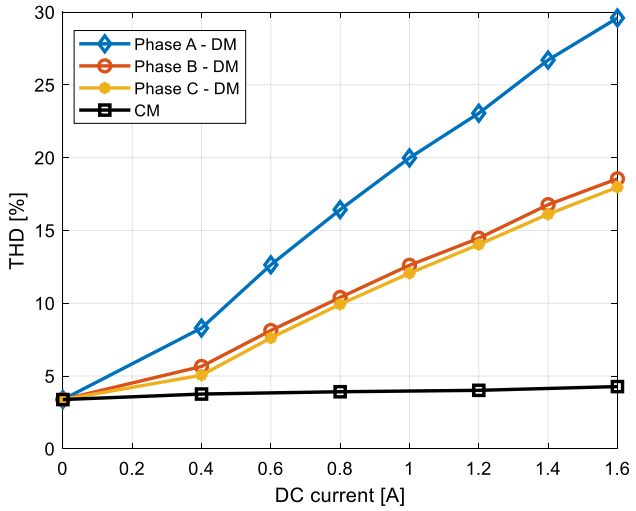

Fig. 14 Current total harmonic distortion (THD) due to different levels of DM and CM dc currents

Detailed harmonic contents due to different levels of DM and CM are presented in Fig. 15. The harmonic current distribution is unbalanced within the three phases for different configurations of DM, which leads to unbalanced winding losses, and more importantly, different stray losses. In contrast, the harmonics of CM are symmetric in the three phases and the magnitudes are much smaller at high frequency.

4.2 Down scaling of transformer

The experiment was carried out on a down-scaled lab transformer, as it is impractical to perform such potentially destructive test on a full-size grid transformer. In principle, the saturation phenomenon is characterized by the flux density in the magnetic core. According to the Ampere's law, the magnetomotive force (defined as NI in ampere-turns) is

$$NI = Hl \tag{5}$$

where N is number of turns, I is current, H is magnetic field strength and l is mean length of the flux path. Then the flux density can be simply expressed by

$$B = \mu H = \mu \frac{NI}{l} \tag{6}$$

where μ is magnetic permeability of the core.

In order to preserve the flux density feature, the down-scaled experiment maintains the same topology of the core and keeps N/l approximately at the same level as full-scale transformer. It has been seen from the lab test that the transformer performance has been degraded at 1.6 A dc current. Such level of dc current (a few ampere) can cause similar saturation for a transformer with 10^5 times larger rating (full-scale transformer, with the same topology and similar N/l).

Despite of the similarity in flux density distribution between the lab transformer and full-scale transformer, it is imperative to highlight the important differences between them.

- Large (full-scale) transformers have sophisticated structural steels such as flitch plates close to the magnetic core which are susceptible to the leakage flux affected by saturation.
- The core material used in a grid (full-scale) transformer is often the grain-oriented (GO) steel, which has higher nominal flux density, lower specific loss and steeper magnetization curve below the knee point, compared to the lab (down-scale) transformer which is made of non-grain-oriented (NGO) steel.
- The rated current in a full-scale transformer is much larger than the lab transformer, so the winding loss generated under the same dc current in a full-scale transformer is not as problematic as the down-scaled one, since the percentage current increase (relative to nominal load current) in a full-scale transformer is much less significant.

The grain-oriented steel (typical core material of a grid transformer) often has steeper magnetization curve (i.e., higher permeability) below the knee point and flatter slope above the knee point (i.e., lower permeability). According to Eq. (6), under the same incremental flux (ΔB), higher magnetization current would be induced in the GO material due to its smaller permeability at saturation. This indicates that the magnetization current with GO material has narrower spike (contents higher frequency current harmonics) than the NGO. As a result, the GO material is more sensitive to dc bias, although it is superior in overall core loss reduction.

5 Conclusions

Measurements of power losses and reactive power in CM and DM reveal that there is a significant difference between the two modes of dc currents in three-phase power transformers. Whether a dc current can cause a damage to a power system or a transformer depends on the mode of the dc current.

- Three-phase, three-limb transformer can withstand much higher CM dc current, compared to DM dc current.
- Power transformers are susceptible to DM dc current regardless of their core topologies, due to low reluctance paths and higher flux density offset.
- The magnetizing current under DM dc current has higher THD level than CM and content higher-order harmonics, resulting in both higher stray loss and higher winding loss.
- The core loss is not significantly influenced by the dc-bias. As demonstrated in Table 3, the core loss even decreases

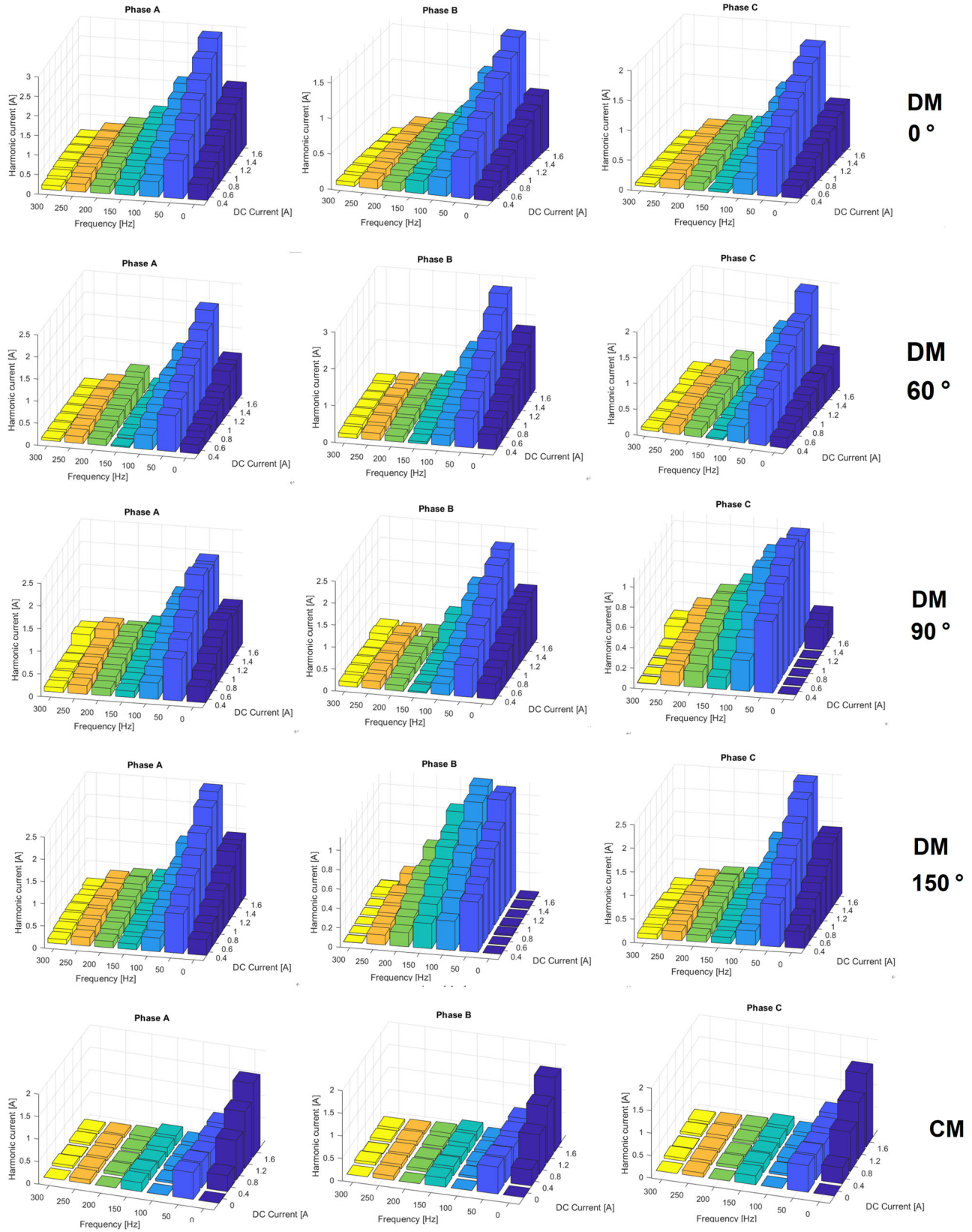

Fig. 15 Current harmonic content due to different levels of DM and CM dc currents

slightly with the dc-bias present, which is in line with the material measurement in [21].

- The power losses caused by high-level DM dc currents depends on dc current distribution in three windings, due to the stray loss redistribution in the iron tank.
- The DM dc currents enhance the reactive power consumption and introduce an unbalanced voltage distribution in the three phases.
- Delta winding can significantly reduce the excessive stray loss (and noise) caused by the DM dc currents, as long as a proper rating is chosen for the delta winding.

The susceptibility classification of power transformers in the guideline [4] applies only to GICs (CM dc currents in general). It is recommended to verify the performance (noise, harmonic distortion, reactive power and/or temperature rise) of a power transformer regardless of its topology, as long as it is exposed to DM dc currents.

Acknowledgements This work was performed as a part of the project "Thermal Modelling of Transformers" (project number: 255178) funded by the Research Council of Norway, Statnett, Hafslund and Lyse Nett.

Funding Open access funding provided by NTNU Norwegian University of Science and Technology (incl St. Olavs Hospital - Trondheim University Hospital).

References

1. Price P (2002) Geomagnetically induced current effects on transformers. IEEE Trans Power Deliv 17(4):1002–1008. https://doi.org/10.1109/MPER.2002.4312311
2. Pirjola R (2000) Geomagnetically induced currents during magnetic storms. IEEE Trans Plasma Sci 28(6):1867–1873. https://doi.org/10.1109/27.902215
3. Girgis R, Ko CD (1992) Calculation techniques and results of effects of GIC currents as applied to large power transformers. IEEE Trans Power Deliv 7(2):699–705. https://doi.org/10.1109/61.127070
4. IEEE (2015) IEEE guide for establishing power transformer capability while under geomagnetic disturbances, In: IEEE C57.163 2015
5. Jiang Y, Ekström A (1997) General analysis of harmonic transfer through converters. IEEE Trans Power Electron 12(2):287–293. https://doi.org/10.1109/63.558741
6. Larsen EV, Walling RA, Bridenbaugh CJ (1989) Parallel AC/DC transmission lines steady-state induction issues. IEEE Trans Power Deliv 4(1):667–673. https://doi.org/10.1109/61.19259
7. Ulleryd J, Ye M and Moreau G (1998) Fundamental frequency coupling between HVAC and HVDC lines in the Quebec-New England multiterminal system-comparison between field measurements and EMTDC simulations. In: International conference on power system technology (POWERCON). Proceedings (Cat. No.98EX151). https://doi.org/10.1109/ICPST.1998.729013
8. Rayo J (2017) General guidelines for HVDC electrode design. Cigré working group B4-61
9. Gleadow JC, Bisewski BJ and Stewart MC (1993) DC ground currents and transformer saturation on the New Zealand HVDC link In: CIGRÉ international colloquium on high voltage direct current and flexible AC power transmission systems, Wellington, New Zealand
10. Mousavi SA (2012) Electromagnetic modelling of power transformers with DC magnetization. Ph.D. dissertation, Dept. Elect. Eng., KTH Royal Institute of Technology, Stockholm
11. Bozoki B et al (1996) The effects of GIC on protective relaying. IEEE Trans Power Deliv 11(2):725–739. https://doi.org/10.1109/61.489329
12. Gattens P and Waggel RM (1989) Investigation of transformer overheating due to solar magnetic disturbances. In: IEEE special panel session report
13. North American Electric Reliability Council (NERC) (1989) Geomagnetic disturbance. In: North American electric reliability corporation final report, (pp 36–60). www.nerc.com/files/1989-Quebec-Disturbance.pdf
14. Kappenman J et al (1991) GIC mitigation: a neutral blocking/bypass device to prevent the flow of GIC in power systems. IEEE Trans Power Deliv 6(3):1271–1281. https://doi.org/10.1109/61.85876
15. Hu JJ and Bisewski B (2011) Evaluation of coupling between dc and ac transmission lines on the same right-of-way: parametric analysis and mitigation methods. In: Minnesota power systems conference (MIPSYCON)
16. Faugstad K, O'Brien M, Smith M, Zavahir M (2007) An environmental survey on the operation and impact of HVDC electrode. In: CIGRÉ, Osaka, Japan
17. Ding H et al (2011) Analysis of coupling effects on overhead VSC-HVDC transmission lines from AC lines with shared right of way. In: IEEE power and energy society general meeting, MI, USA, 24–28 July 2011. https://doi.org/10.1109/PES.2011.6038904
18. Sharifabadi K, Harnefors L, Nee HP, Norrga S, Teodorescu R (2016) Design, control, and application of modular multilevel converters for HVDC transmission systems. Wiley-IEEE Press, Chichster
19. The Math Works, Inc (2020) MATLAB. (Version 2020a) [Computer Software], https://www.mathworks.com/
20. Savini A, Turowski J (1988) Electromagnetic fields in electrical engineering. Plenum Press, New York, pp 119–127
21. Wang W, Nysveen A, Magnusson N (2020) Apparatus for loss measurements under multidirectional and dc-bias flux in electrical steel laminations. Rev Sci Instrum 91(8):084705